

Sharp and smooth boundaries of quantum Hall liquids

C. de C. Chamon and X. G. Wen

Department of Physics, Massachusetts Institute of Technology, Cambridge, Massachusetts 02139

(Received 6 October 1993)

We study the transition between sharp and smooth density distributions at the edges of quantum Hall liquids in the presence of interactions. We find that, for strong confining potentials, the edge of a $\nu = 1$ liquid is described by the $Z_F = 1$ Fermi-liquid theory, even in the presence of interactions, a consequence of the chiral nature of the system. When the edge confining potential is decreased beyond a point, the edge undergoes a reconstruction and electrons start to deposit a distance ~ 2 magnetic lengths away from the initial quantum Hall liquid. Within the Hartree-Fock approximation, a new pair of branches of gapless edge excitations is generated after the transition. We show that the transition is controlled by the balance between a long-ranged repulsive Hartree term and a short-ranged attractive exchange term. Such a transition also occurs for quantum dots in the quantum Hall regime and should be observable in resonant tunneling experiments. We find that the edge theory for sharp edges also applies to smooth edges (i.e., reconstructed edges) once the additional pairs of edge branches are included. Electron tunneling into the reconstructed edge is also discussed.

I. INTRODUCTION

In fractional quantum Hall (FQH) states there are no bulk gapless excitations; the only gapless modes are edge states, which are responsible for nontrivial transport properties at low temperatures. Edge states arise naturally in real samples, as the two dimensional electron gas (2DEG) is confined in a finite region. The manner in which the 2DEG is confined determines the structure of the electronic density on the borders of the sample, and rich structures may appear.

If we ignore the electron correlations, the electronic density near the edges of a $\nu = 1$ liquid can be determined from an electrostatic consideration. For a typical smooth confining potential in experimental devices, the electron density changes smoothly from $\nu = 1$ to $\nu = 0$ in a range of order a few thousand angstroms. The structure of these smooth edges has been studied mainly by focusing on the electronic density distribution at large length scales, where it is reasonable to use a semiclassical approach.²⁻⁴ In this approach, one calculates the stable electron density distribution $n(x)$ by minimizing the electrostatic energy

$$\frac{e^2}{2\epsilon} \int d^2x d^2y \frac{n(x)n(y)}{|x-y|} + \frac{e}{\epsilon} \int d^2x n(x)V(x). \quad (1)$$

In a refined consideration, one assumes that the internal energy of the 2DEG $u(n)$ has cusps for n corresponding to fractional filling factors as a consequence of the correlation. In this case, strips of compressible and incompressible FQH states may be formed between the $\nu = 1$ and $\nu = 0$ regions.^{1,2} An improved calculation using the Hartree-Fock approximation was done in Ref. 5 at finite temperature, which agrees very well with the electrostatic calculation.⁴

In the opposite extreme of a strong confining potential,

the electron density varies sharply at the edge, leaving no room for the formation of compressible or incompressible strips. One needs to use a quantum mechanical treatment to determine the structures of the edge. In the Landau gauge, the states in the first Landau level are labeled by momentum k_x . If the electron interaction is much weaker than the confining potential, electrons simply fill all the energy levels up to a "Fermi" momentum k_F [i.e., the electron occupation number takes a form $n_{k_x} = \theta(k_F - k_x)$]. In this case the edge electrons are described by a chiral Fermi liquid in which electrons only propagate in one direction. The electronic density profile of the edge $\langle n(y) \rangle$ can be obtained from the momentum occupation $\langle n_{k_x} \rangle$ by a convolution with a Gaussian function.

One naturally questions how the above picture changes when the electron-electron interactions are included, and how the sharp edge picture evolves into the smooth edge picture as the edge potential becomes smoother. As an interacting 1D system, the Fermi edge of the $\nu = 1$ state may have the following possible singularities displayed in Fig. 1, such as a Fermi liquid singularity, with a $Z_F = 1$ discontinuity [Fig. 1(a)] (Z_F is the discontinuity of the momentum occupation n_{k_x} across the Fermi point k_F) or a renormalized $Z_F < 1$ discontinuity [Fig. 1(b)], or a Luttinger liquid singularity [Fig. 1(c)]. One scenario is that the sharp edge and the smooth edge are connected continuously by the distributions in Fig. 1(b) or 1(c). As the edge potential becomes smoother, the occupation distributions in Figs. 1(b) and 1(c) also get smoother. According to this picture, the smooth edge of the $\nu = 1$ state contains one branch of gapless edge excitations which is described by a renormalized Fermi liquid. The smoother the edge, the stronger the renormalization. However, the calculations presented in this paper suggest a new scenario for some natural confining potentials. We find that the chiral nature of this one dimensional system plays an

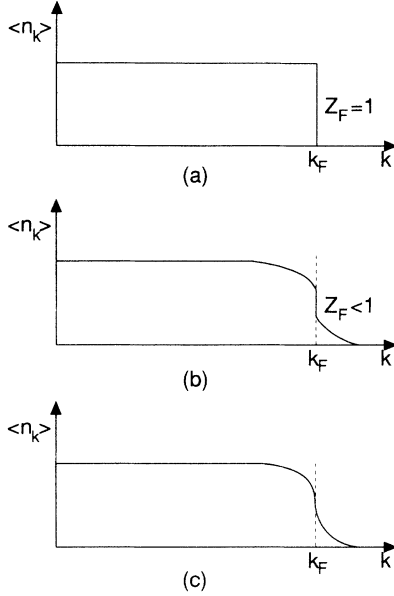


FIG. 1. Possible singularities for the momentum occupation distribution of a $\nu = 1$ state: (a) $Z_F = 1$ Fermi-liquid singularity, (b) $Z_F < 1$ Fermi-liquid singularity, and (c) Luttinger liquid singularity.

important role in determining the form of the singularity. Due to the chirality (i.e., the fact that electrons near the edge propagate only in one direction), the $Z_F = 1$ edge is very stable. Figure 1(a) correctly describes the edge structure for a range of edge potentials even for interacting electrons. However, as the edge potential is smoothed beyond a certain point, the edge undergoes a reconstruction. The occupation distribution in Fig. 1(a) changes into the one in Fig. 2, which contains three Fermi points. The occupation $\langle n_k \rangle$ has algebraic singularities at these Fermi points. The addition of two more Fermi points to the momentum occupation is accompanied by the generation of a pair of edge branches moving in opposite directions. This new scenario has received some support from exact calculations on small systems.

In this paper we focus on the structure of the electronic occupation density distribution at the boundary of a $\nu = 1$ liquid in the presence of interactions. We work with a Hilbert space restricted to the first Landau

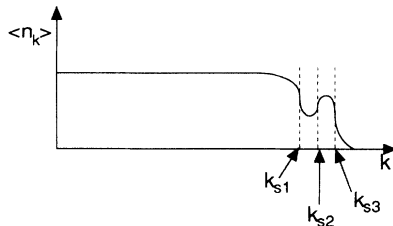


FIG. 2. Momentum occupation distribution after reconstruction, with three singularities. The addition of two singularities corresponds to the addition of two branches of opposite moving edge excitations.

level, and in the main part of the paper we assume that the spins are fully polarized. The droplet is confined by its interaction with an underlying positive background (one way to introduce a confining potential). The paper is organized as follows. In Sec. II we introduce the 1D interacting version for the problem and discuss the importance of chirality in determining the structure of the edge singularity. In Sec. III we present exact numerical results for small systems, which support the picture that, before a discontinuous transition occurs, the chiral edge system is reasonably well described within the Hartree-Fock approximation. In Sec. IV we study the effects of this transition for quantum dots. The experimental consequences of the edge reconstruction in quantum dot systems are discussed. Finally, in Sec. V we investigate the consequences of the transition on the dynamics of edge excitations, and in Sec. VI the consequences to electron tunneling into the reconstructed edges.

II. THE 1D INTERACTING MODEL AND CONSEQUENCES OF CHIRALITY

A system of interacting particles in a 2D QH droplet can be mapped into a one dimensional problem by enumerating the single particle wave functions of the first Landau level. The Hamiltonian of the interacting theory is

$$H = \sum_{\lambda, \lambda'} \epsilon_{\lambda, \lambda'} c_{\lambda}^{\dagger} c_{\lambda'} + \sum_{\lambda_1, \lambda_2, \lambda_3, \lambda_4} V_{\lambda_1, \lambda_2, \lambda_3, \lambda_4} c_{\lambda_1}^{\dagger} c_{\lambda_2} c_{\lambda_3}^{\dagger} c_{\lambda_4}, \quad (2)$$

where

$$\epsilon_{\lambda, \lambda'} = \int dx_1^2 dx_2^2 \rho(\vec{x}_1) V(|\vec{x}_1 - \vec{x}_2|) \phi_{\lambda}^*(\vec{x}_2) \phi_{\lambda'}(\vec{x}_2),$$

$$V_{\lambda_1, \lambda_2, \lambda_3, \lambda_4} = \frac{1}{2} \int dx_1^2 dx_2^2 \phi_{\lambda_1}^*(\vec{x}_1) \phi_{\lambda_2}(\vec{x}_1) \times V(|\vec{x}_1 - \vec{x}_2|) \phi_{\lambda_3}^*(\vec{x}_2) \phi_{\lambda_4}(\vec{x}_2).$$

The dispersion $\epsilon_{\lambda, \lambda'}$ is determined by a background charge $\rho(\vec{x})$, which we use to control the confining potential. The ϕ_{λ} 's are the single particle wave functions, labeled by the quantum number λ . For example, in the symmetric gauge, λ stands for the angular momentum quantum number m , with $\phi_m(x, y) = \frac{1}{\sqrt{\pi}} \frac{z^m}{\sqrt{m!}} e^{-|z|^2/2}$ and $z = \frac{x+iy}{\sqrt{2}}$ (throughout the paper we work in units of magnetic length $l_B = 1$). The wave packet ϕ_m is centered in a circle of radius $R = \sqrt{2m}$. In the Landau gauge, λ denotes the linear momentum in the x direction k_x , with $\phi_{k_x}(x, y) = \frac{1}{(\sqrt{\pi}L)^{1/2}} e^{ik_x x} e^{-(y-k_x)^2/2}$, and the wave packet ϕ_{k_x} is centered at $y = k_x$ (L is the size of a system subject to periodic boundary conditions).

Let us consider for now backgrounds $\rho(\vec{x})$ that are invariant under certain symmetry transformations, such as rotations (if we are studying a circular droplet, using the symmetric gauge) or translations along the x direction (if

we are studying a long strip, using the Landau gauge). In this case we have $\epsilon_{\lambda,\lambda'} = \epsilon_{\lambda} \delta_{\lambda,\lambda'}$. Impurities break such symmetries, and their effect will be considered later in the paper. Because the interaction $V(|\vec{x}_1 - \vec{x}_2|)$ depends only on the distance between \vec{x}_1 and \vec{x}_2 , it is also invariant under these symmetries, and thus we can rewrite the Hamiltonian as

$$H = \sum_{\lambda} \epsilon_{\lambda} c_{\lambda}^{\dagger} c_{\lambda} + \sum_{\delta,\lambda,\lambda'} V(\delta, \lambda, \lambda') c_{\lambda+\delta}^{\dagger} c_{\lambda} c_{\lambda'}^{\dagger} c_{\lambda'+\delta} \quad (3)$$

It is this 1D interacting model that will be the basis of our study of the $\nu = 1$ droplet. The question we want to address is how to determine the ground state occupation number $\langle c_{\lambda}^{\dagger} c_{\lambda} \rangle$ for this theory.

Without loss of generality, let us focus now on the problem of a strip with length L and periodic boundary conditions (equivalently, a cylinder of circumference L), using the Landau gauge. The QH fluid lies on the surface of the cylinder, between its left (L) and right (R) boundaries (see Fig. 3).

In a typical 1D interacting theory we have non-Fermi-liquid behavior; the Fermi discontinuity is destroyed by the interactions, and the system is better described as a Luttinger liquid. Notice, however, that the Hamiltonian in Eq. (3) has a peculiar difference from the usual 1D Hamiltonian of an interacting system in the sense that the effective scattering potential V depends not only in the momentum transferred δ , but also in the momentum configuration (i.e., λ and λ') of the scattered particles. The Luttinger liquid behavior is caused by the coupling between particle-hole excitations in the two distinct Fermi points. Now, for our system described in Eq. (3), the two Fermi points correspond to λ_L and λ_R , at the two boundaries of our droplet. These two points are spatially separated, and the matrix elements for coupled particle-hole excitations near these points should go to zero as the distance between the boundaries is increased. In the limit of infinite separation, the two edges are decoupled, and we can describe the system as containing two different types of fermions R and L with one Fermi point each. More precisely, we can describe the particles as being in a Dirac sea that is filled as we move inwards to the bulk. Indeed, in topologies such as a simply connected droplet, like a disk, we only have one boundary,

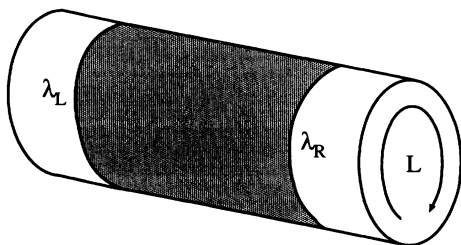


FIG. 3. Cylindrical geometry, equivalent to a strip of length L and periodic boundary conditions, where it is convenient to use the Landau gauge. The QH liquid (shaded area) lies on the surface of the cylinder, between its left and right edges at λ_L and λ_R .

and the Dirac sea description is exact. Such theories fall within what we call “chiral Luttinger liquids.”

The 1D chiral theory has a special property that the occupation distribution of the ground state can have a Fermi discontinuity (Fermi liquid) *even in the presence of interactions*. In fact, for certain values of interaction strength and single particle dispersion, the ground state may have a perfect Fermi distribution with $Z_F = 1$. This is because the momentum occupation with $Z_F = 1$ is always an eigenstate of the *interacting* Hamiltonian (3) in the limit of infinitely separated edges. This is easier seen in the filled Dirac sea description of the L and R fermions. Take, for example, the R branch, for which the unique minimum total momentum eigenstate is the one that has all single particle levels to the left of the edge occupied. Because total momentum commutes with the Hamiltonian, and this state is the only one with minimum total momentum, it must also be an eigenstate of energy, possibly the ground state for some edge potential. Notice that the occupation distribution of this state corresponds exactly to a $Z_F = 1$ Fermi-liquid occupation. One should contrast this case with a nonchiral 1D system, where clearly the Fermi gas distribution is an eigenstate of zero total momentum, but it is not the only one, and thus not necessarily an eigenstate of energy. Again, chirality plays a key role.

The next step is to understand how the occupation distribution evolves as we smooth the confining potential. One way to assemble a sharp distribution is by simply laying the electron gas on top of a similarly sharp positively charged background, and one way to try to destroy this sharp distribution is to smooth the positive background. Notice that the perturbation we include by changing the background is not in the form of an additional interaction between the particles, but of a change in the one particle dispersion ϵ_{λ} . We will show that the occupation distribution has the tendency to remain sharp, due to a balance between a repulsive long-range Hartree term and an attractive short-range Fock term, and also due to the special stability of the $Z_F = 1$ chiral Fermi liquid. The sharp distribution eventually becomes unstable, and the Fermi surface is destroyed, as a lump of particles detach and form two more edges which destroy the chirality. We will show that the Hartree-Fock approximation seems to contain the relevant ingredients to describe this transition.

III. EXACT RESULTS FOR SMALL SYSTEMS

In the Landau gauge, the dispersion due to the background charge, and the matrix elements V in Eq. (3) for

$$\epsilon_k = \frac{e^2}{\epsilon} \int_{-\infty}^{\infty} dy' \rho(y') \int_{-\infty}^{\infty} dy \frac{e^{-(y-k+y')^2}}{\sqrt{\pi}} \ln y^2 \quad (4)$$

and

$$V(q, \Delta k) = \frac{e^2}{\epsilon} \frac{1}{L} \frac{e^{-q^2/2}}{\sqrt{2\pi}} \int_{-\infty}^{\infty} dy e^{-(y-\Delta k)^2/2} K_0(qy), \quad (5)$$

where e is the electron charge, ϵ is the dielectric constant, q is the momentum transfer [δ in Eq. (3)], $\Delta k = k - k'$, ρ is the positive background density, and K_0 is a modified Bessel function. Notice that $e^2/\epsilon l_B$ (or e^2/ϵ , as we use units of $l_B = 1$) is the natural energy scale in the problem. In particular, the Hartree-Fock effective two body potential between two particles with momenta k_1 and k_2 is given by

$$V_{\text{HF}}(k_1, k_2) = V_H(|k_1 - k_2|) + V_{\text{ex}}(|k_1 - k_2|), \quad (6)$$

where the Hartree and exchange terms are obtained from Eq. (5) by setting $q \rightarrow 0$, $\Delta k = k_1 - k_2$ and $q = k_1 - k_2$, $\Delta k = 0$, respectively (with a factor of -1 for the exchange):

$$V_H(|k_1 - k_2|) = -\frac{1}{2L} \frac{e^2}{\epsilon} \int_{-\infty}^{\infty} dy \frac{e^{-(y-k_1+k_2)^2/2}}{\sqrt{2\pi}} \ln y^2, \quad (7)$$

$$V_{\text{ex}}(|k_1 - k_2|) = -\frac{1}{2L} \frac{e^2}{\epsilon} e^{-(k_1-k_2/2)^2} K_0 \left[\left(\frac{k_1-k_2}{2} \right)^2 \right].$$

We subtracted a logarithmic divergence from the Hartree term ($\sim \ln q|_{q \rightarrow 0}$), which is independent of k_1 and k_2 , and thus simply contributes to a constant in the energy. The Hartree contribution to the effective two body potential V_H is repulsive and long ranged, whereas the one from exchange V_{ex} is attractive and short ranged. We will show that it is a balance between these two effective interactions that controls the short length scale behavior of the density distribution.

We will proceed by first presenting exact numerical results for a small system and then using these results to justify a picture that the short length scale behavior of the density distribution is controlled by the Hartree-Fock terms.

We study the edge structure of a system that we divide into “edge” and “bulk” electrons (see Fig. 4). We consider just one edge, say, the R edge, and assume the bulk extends to infinity in the opposite direction. The occupation of the bulk levels is fixed to be 1. Doing so, we can concentrate all the computations on the edge, as the effect of bulk electrons is simply reduced to a contribution to the one particle dispersion of the edge electrons. Such division presents no harm, as long as the edge excitations

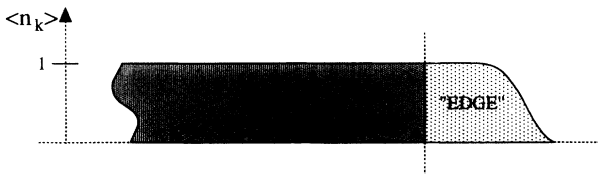


FIG. 4. The $\nu = 1$ droplet is divided into “bulk,” where all the states are fully occupied, and “edge,” in which states can be partially occupied. The division allows one to focus the computations solely on the edge electrons, with the bulk simply contributing to the one particle dispersion. This sort of division is not unique, as one can adjust the position of the boundary between the two regions; this boundary can be moved as long as the sites on the edge side of it are all fully occupied.

under consideration do not change the bulk occupation.

Consider a strip geometry with $L = 20l_B$ and periodic boundary conditions (cylinder). The edge is composed of 10 electrons in 20 single particle states. We start with a sharp background and smooth it by changing the width w in which the density drops from the bulk value ($\rho = 1/2\pi$ for $\nu = 1$) to zero (see Fig. 5). The bulk electrons contribute to an additional term in the dispersion. The effect of adding a variation in the positive charge density over a length scale w can be thought of as simply superimposing a dipole to the effective edge potential for a sharp edge, as shown in Fig. 5.

Figure 6 displays the energy levels for different total momentum K of the edge electrons (the sites, numbered from 1 to 20, are assigned $k = 0-19$). For $w < 8l_B$ the ground state has $K = 45$, i.e., all the electrons are packed up to one side and the edge is described by the $Z_F = 1$ Fermi liquid. For $w = 9l_B$ the ground state is no longer the sharp configuration with minimum $K = 45$, but has moved to a configuration with $K = 60$ (see Fig. 7). The occupation number distribution is shown in Fig. 8 for $w = 9l_B$ and $10l_B$. Notice the formation of a lump of electrons distant $\sim 2l_B$ from the bulk (for $L = 20$, $\Delta k = 1$ corresponds to a distance $2\pi/L \sim 0.314l_B$).

The exact calculation for a small system seems to indicate that the sharp edge is robust against the smoothing of the background charge, up to a point where there is a transition, and the density redistributes. We will show that the robustness of the sharp edge is a consequence of the attractive exchange, which tends to keep the edge packed. Eventually, as the strength of the dipole result-

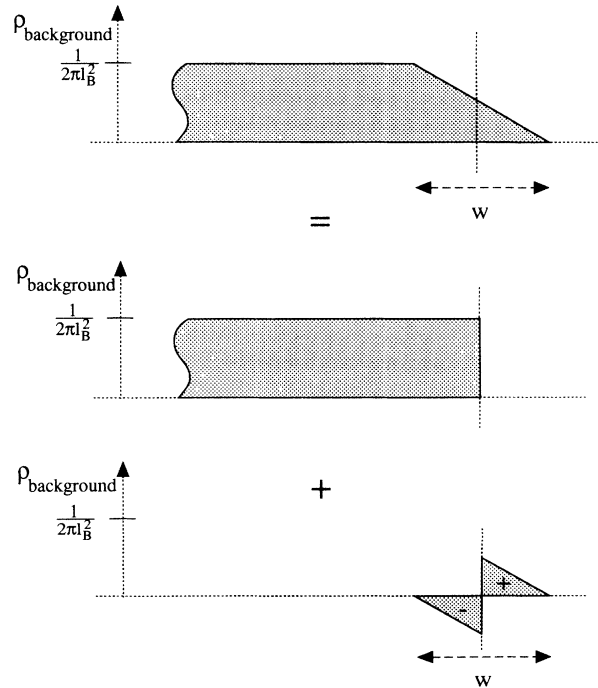


FIG. 5. Smoothed background charge density, which over a width w drops from its bulk value to zero. Such density can be written as the superposition of a sharp density profile to a dipole term, which is used to tune the confining potential as function of w .

ing from the smoothing of the background is increased, the short-range attraction due to exchange can no longer sustain the edge sharp and a lump of the electrons splits and forms a “puddle” near the minimum of the effective potential seen by the QH liquid. Let us illustrate the point above by calculating the effective single particle energy within the Hartree-Fock approximation for the distribution that has occupied levels for all negative momenta, i.e., a sharp R edge (we have centered the coordinate system on the edge):

$$\epsilon(k) = \epsilon_k + \Sigma_H(k) + \Sigma_{\text{ex}}(k), \quad (8)$$

where

$$\epsilon_k = \frac{e^2}{\epsilon} \int_{-\infty}^{\infty} dy' \rho(y') \int_{-\infty}^{\infty} dy \frac{e^{-(y-k+y')^2}}{\sqrt{\pi}} \ln y^2,$$

$$\Sigma_H(k) = -\frac{e^2}{\epsilon} \int_{-\infty}^0 \frac{dk'}{2\pi} \int_{-\infty}^{\infty} dy \frac{e^{-(y-k+k')^2/2}}{\sqrt{2\pi}} \ln y^2,$$

$$\Sigma_{\text{ex}}(k) = -\frac{e^2}{\epsilon} \int_{-\infty}^0 \frac{dk'}{2\pi} e^{-(k-k')^2/2} K_0 \left[\left(\frac{k-k'}{2} \right)^2 \right].$$

One should notice that the electronic occupation number $n_k = \langle c_k^\dagger c_k \rangle$ differs from the electronic charge density

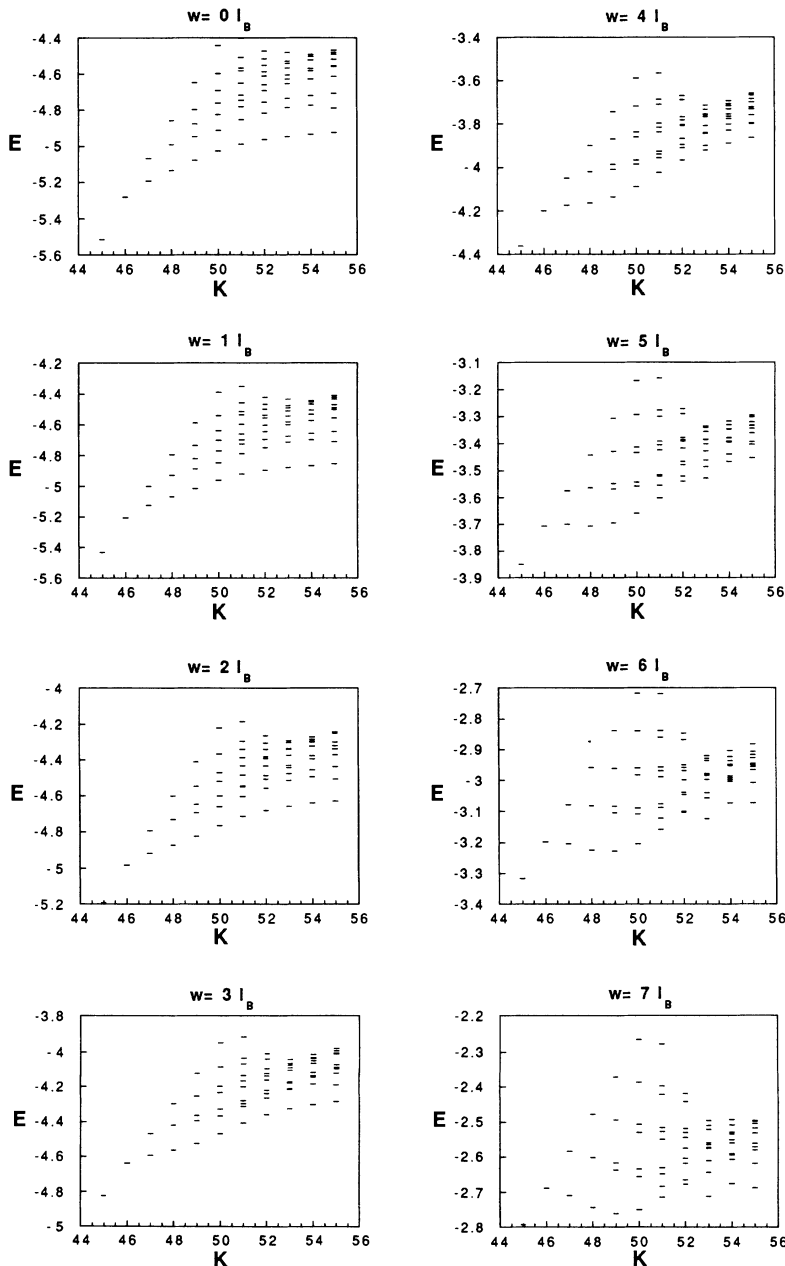


FIG. 6. Energy eigenstates obtained as function of the total momentum K of the edge electrons for values of w ranging from $0l_B$ to $7l_B$. Notice that the ground state for this range has $= K = 45$, the minimum momentum configuration for 10 electrons (the 20 sites used in the calculation are assigned k values from 0 to 19). Also notice that the energy levels of states of higher K are pulled down as w increases.

$n(y) = \langle c^\dagger(y)c(y) \rangle$. The latter is obtained from the former by a convolution with a Gaussian function of variance $\sigma^2 = 1/2$ (the single level charge distribution). With this in mind, one can show that the background density that cancels the electronic charge density is exactly the one that makes $\epsilon_k + \Sigma_H(k) = 0$, as it should be expected. A sharp background charge distribution as shown in Fig. 5 makes a sharp electronic occupation distribution even more stable, as we have an extra dipole term, resulting from the difference between a sharp positive charge background and the electronic charge density of a sharp occupation distribution, and which favors the levels with negative k to remain occupied.

As we change the background configuration, we alter

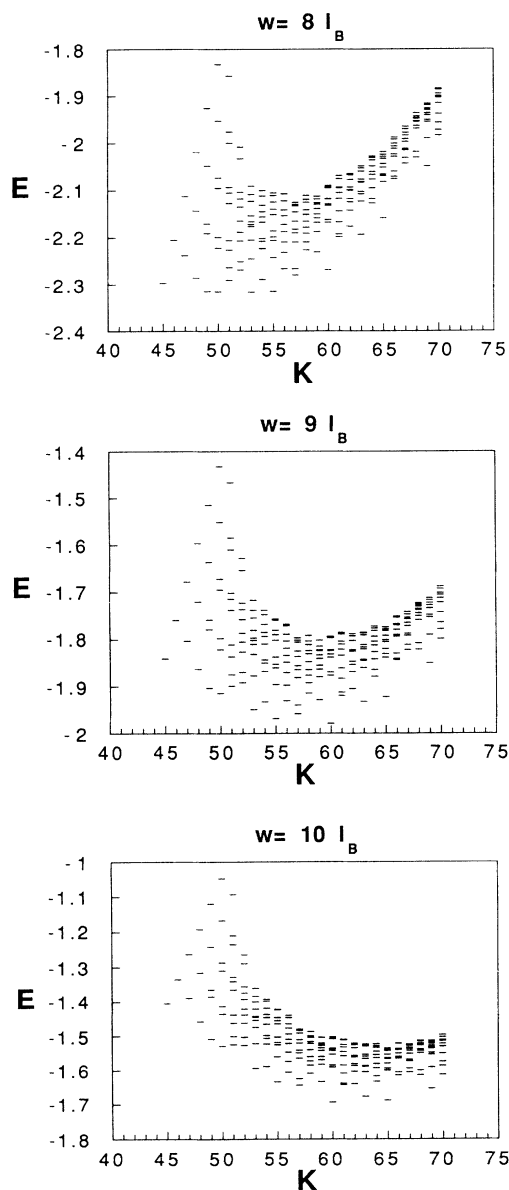


FIG. 7. For $w \geq 8l_B$ the ground state configuration is no longer the sharp edge distribution. The transition occurs near $w = 8l_B$, and for $w = 9l_B$ is already fully developed, with the ground state momentum moved to $K = 60$.

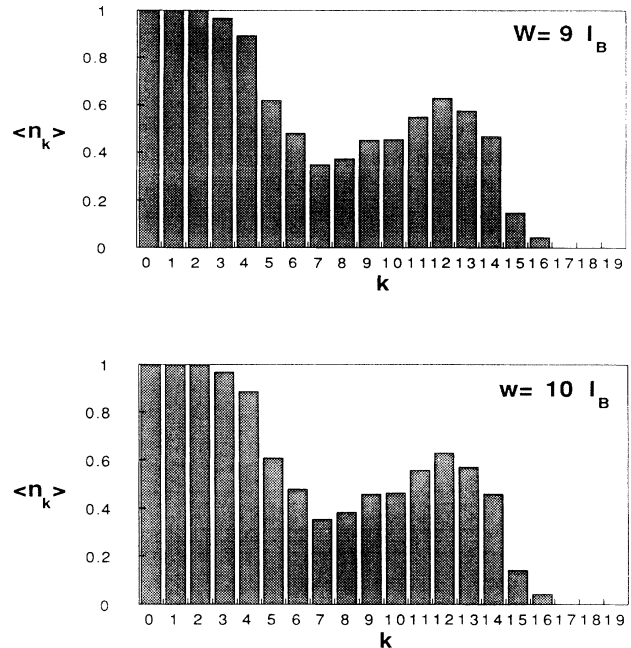


FIG. 8. Occupation numbers for the ground state past the transition, for $w = 9l_B$ and $10l_B$. Notice how a lump of density moves away from the main body of QH fluid. This density profile (which goes from its bulk value to zero by first decreasing, then increasing, and finally decreasing again) is the signature of the existence of now three singularities, and thus three branches of edge excitations.

the one particle dispersion ϵ_k . For the stability of this edge it is necessary that the effective single particle energy of any unoccupied level be higher than the one of any occupied level. Figure 9 shows the effective single particle energy for unoccupied levels for different values of the parameter w , which measures the width which it takes the background to decrease from its bulk value to

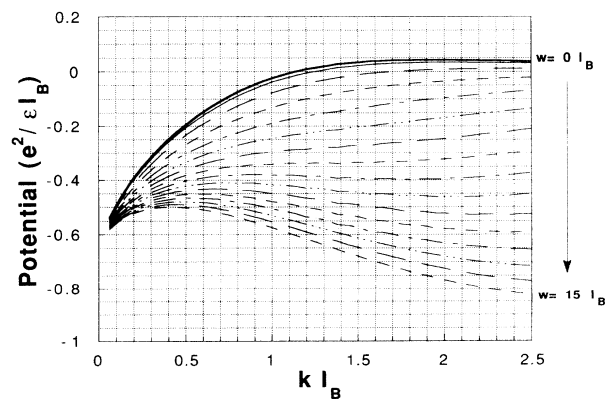


FIG. 9. The effective single particle potential calculated within the Hartree-Fock approximation for different widths w , decreasing from $0l_B$ to $15l_B$ in steps of $1l_B$. Notice that starting at $w \sim 11l_B$, the condition for stability of a sharp edge is violated, as there are locations with smaller effective potential than the one at the edge of the sharp occupation density.

zero. The potential obtained for $w = 0l_B$ is primarily due to the exchange term, which stabilizes a sharp edge. The exchange potential is short ranged, reaching zero within $\sim 1.5 - 2l_B$; the overshoot for $w = 0l_B$ is due to the dipole which results from the difference between a sharp positive charge background and the electronic charge density of a sharp occupation distribution, as mentioned previously, whose contribution decays to zero as $1/|k|$ for large $|k|$. For $w \sim 11l_B$ the condition for stability is violated (the higher value for the w that marks the transition, as compared to the small system result, can be regarded as due to a finite size effect, to the Hartree-Fock approximation, or to both). It is then more advantageous to move electrons to the minimum $\epsilon(k)$ locations. A simple picture is that particles start to escape from the sharp edge and start to deposit at a distance of order $\sim 2l_B$ away from the initial boundary. This separated lump brings in two new boundaries into the problem. These new boundaries break our previous chiral geometry, as we now have three Fermi points finitely separated. The three Fermi points describe two right-moving branches and one left-moving branch of edge excitations. From this point on one should expect that the interactions will destroy the Fermi-liquid singularities, and we will have three Luttinger singularities.

Notice that we said the necessary condition for the stability of the sharp edge is that $\epsilon(k)$ be larger for unoccupied states than for occupied states. But we have not yet argued it is sufficient. It is possible that even if this condition is satisfied one can have a ground state for the interacting problem different from the sharp edge, as the energy could be lowered by rearranging many particles. Worse, it is possible that the hopping terms, which couple different states in configuration space (and are not included within Hartree-Fock), would completely mod-

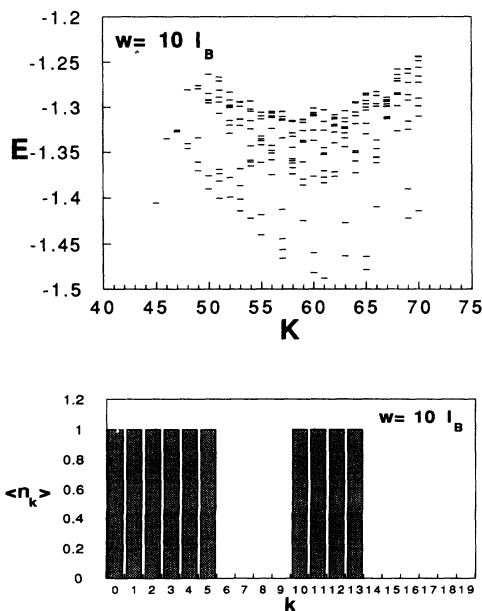


FIG. 10. Energy levels and occupation numbers for $w = 10l_B$ calculated within the Hartree-Fock approximation (the hopping or off-diagonal elements were suppressed).

ify the picture. In particular, the Hartree-Fock approximation does not allow the distributions in Figs. 1(b) and 1(c). Therefore, we cannot use the Hartree-Fock calculation alone to judge which of the distributions in Figs. 1 and 2 is realized after the transition. However, the exact diagonalization results for small systems that we have presented support the picture described in Fig. 2. This suggests that the transition is mainly controlled by Hartree-Fock terms and that the conclusions depicted from the single particle potential obtained within Hartree-Fock seem to be qualitatively correct. Certainly we cannot rule out the possibility that Figs. 1(b) and 1(c) might be realized for some other interaction and edge potential.

To finalize this section, we present in Fig. 10 the spectrum and occupation numbers calculated for the small system with $w = 10l_B$, but now within the Hartree-Fock approximation (the hopping or off-diagonal elements were suppressed). Compare the spectrum to the exact diagonalization for $w = 10l_B$ displayed in Fig. 7. The occupation numbers in the Hartree-Fock approximation suggest the separation of part of the density from the main fluid and the appearance of two more singularities. The hopping elements would take charge in redistributing the density, modifying the form of the singularity.

IV. THE EDGE RECONSTRUCTION FOR QUANTUM DOTS

The effect we describe in this paper is not particular to large systems. In fact, the exact results for small systems, which we used to support the Hartree-Fock picture, directly indicate that the transition occurs for finite systems. The edge density redistribution is a consequence of the balance between the confining potential, the repulsive Hartree term, and the short-ranged exchange, all of these present regardless of the size of the system.

Quantum dots are innately interesting systems for observing this transition. To begin with, because the number of electrons is small, the redistribution will involve a substantial part of the total number of particles in the dot, which can then be considered not simply an edge effect, but, in a way, a bulk effect as well. Second, experiments on resonant tunneling into quantum dots in the FQH regime should be sensitive to a transition involving a redistribution of the particle density both because the energies of adding one electron to the dot on both sides of the transition should differ (which can be measured by the position of the resonant peaks) and because a change in the size of the dot will change the coupling to the probe leads as well. Third, the transition can be driven by altering the confining potential, either changing the voltage on a back gate or changing the magnetic field (which varies the radii of the orbits, and consequently the potential seen by each orbit).

In this section we study some of the consequences of the transition as applied to quantum dots. We study systems with total numbers of particles up to $N_p = 70$. We will use only the Hartree-Fock matrix elements because the system is not small enough for exact diagonalization and

the Hartree-Fock approximation seemed to contain the essential elements to describe the transition.

The energy eigenstates of the Hamiltonian in Eq. (3) are also eigenstates of total momentum. The true ground state is a superposition of different occupation number states in Fock space, all of them with the same total momentum. We will call hopping elements the terms in the Hamiltonian that couple different states in Fock space. The Hartree and Fock terms couple a configuration in Fock space to itself. Within the Hartree-Fock approximation, i.e., neglecting the hopping terms in the Hamiltonian, any occupation number state is an energy eigenstate. Finding the ground state is then equivalent to determining the configuration of particles that minimizes a classical energy function. Notice that within the Hartree-Fock approximation all $\langle c_\lambda^\dagger c_\lambda \rangle$ are equal to either 0 or 1.

We focus on a disk geometry, which is more appropriate for describing a dot. The single particle states are labeled by the angular momentum quantum number. The matrix elements are given by

$$V_{m1,m2,m3,m4} = \langle m1 m3 | \hat{V} | m2 m4 \rangle, \quad (9)$$

where the state $|m m'\rangle$ stands for a particle in the level labeled by m and another in the level m' [$\langle z_1, z_2 | m m'\rangle = \phi_{m,m'}(z_1, z_2) = \frac{1}{\sqrt{\pi}} \frac{z_1^m z_2^{m'}}{\sqrt{m! m'}} e^{-\frac{|z_1|^2 + |z_2|^2}{2}}$, with $z_{1,2} = \frac{z_{1,2} + iy_{1,2}}{\sqrt{2}}$]. The matrix elements in the classical energy function that couple states m and m' are obtained from the Hartree and Fock terms:

$$V_{m,m'}^{\text{HF}} = V_{m,m,m',m'} - V_{m',m,m,m'}. \quad (10)$$

To obtain these coefficients it is easier to work in a basis in which \hat{V} is diagonal. The $|l, n\rangle$ basis, in which $\langle z_1, z_2 | l, n\rangle = \frac{1}{\sqrt{\pi}} \frac{z_+^n z_-^l}{\sqrt{n! l!}} e^{-\frac{|z_+|^2 + |z_-|^2}{2}}$, where $z_{\pm} = \frac{z_1 \pm z_2}{\sqrt{2}}$, is such that $\langle l, n | \hat{V} | l', n'\rangle = V(l) \delta_{l,l'} \delta_{n,n'}$. For the Coulomb interaction we have

$$\begin{aligned} V(l) &= \frac{1}{2} \frac{e^2}{\epsilon l_B} \int \frac{dz_+^2 dz_-^2}{\pi^2} \frac{1}{2|z_-|} \frac{|z_+|^{2n} |z_-|^{2l}}{n! l!} \\ &\quad \times e^{-|z_+|^2} e^{-|z_-|^2} \\ &= \frac{e^2}{\epsilon l_B} \frac{1}{4} \frac{\Gamma(l+1/2)}{\Gamma(l+1)} \end{aligned} \quad (11)$$

The Hartree and exchange terms are obtained, respectively, using

$$\langle m m' | \hat{V} | m m' \rangle = \sum_{l,n} V(l) |\langle m m' | l, n \rangle|^2 \quad (12)$$

and

$$\langle m m' | \hat{V} | m' m \rangle = \sum_{l,n} (-1)^l V(l) |\langle m m' | l, n \rangle|^2. \quad (13)$$

The confining potential is assumed to be parabolic, $\epsilon(r) = \frac{1}{2} k r^2$, with r the distance from the center of the dot and k the strength of the confining potential. It is convenient to write $k = \alpha_0 \frac{e^2}{\epsilon l_B} l_B^{-2}$, so that α_0 is a dimensionless parameter, maintaining $e^2/\epsilon l_B$ and l_B as our,

respectively, energy and length units. The single particle dispersion is given by

$$\begin{aligned} \epsilon_m &= \frac{1}{2} \alpha_0 \frac{e^2}{\epsilon l_B} \int \frac{dz^2}{\pi} 2|z|^2 \frac{|z|^{2m}}{m!} e^{-|z|^2} \\ &= \alpha_0 \frac{e^2}{\epsilon l_B} \frac{\Gamma(m+2)}{\Gamma(m+1)} = \alpha_0 \frac{e^2}{\epsilon l_B} (m+1). \end{aligned} \quad (14)$$

The energy function that must be minimized is

$$\mathcal{E} = \sum_m \epsilon_m n_m + \sum_{m,m'} V_{m,m'}^{\text{HF}} n_m n_{m'}, \quad (15)$$

where the n_m 's are 0 or 1, constrained to $\sum n_m = N_p$, the total number of particles. We obtained numerically $V_{m,m'}^{\text{HF}}$ for the first 80 levels ($0 \leq m, m' \leq 79$), and searched for the minimum of \mathcal{E} for different values of N_p and α_0 . We find that, depending on these parameters, the minimum energy configuration switches from a compacted to a separated droplet.

In Fig. 11 we display the occupation of the orbits as function of α_0 for $N_p = 60$ (occupied orbits are displayed in black and unoccupied ones in white). For strong confining potentials the occupied levels are the ones with minimum angular momentum. As the confining strength is decreased, there is a transition and unoccupied levels inside the dot appear. After the transition, hopping elements become important and take charge in redistributing the occupation, which can then have partially filled levels. Figure 12 displays the orbital occupation for fixed α_0 , with N_p varying from 70 to 30 electrons, where there is also a transition, with a separated droplet for smaller systems. This sort of instability for the compacted dots, with the formation of holes in the bulk, has been discussed in Ref. 6. There the self-energy was calculated for a compacted dot and the stability criterion is that

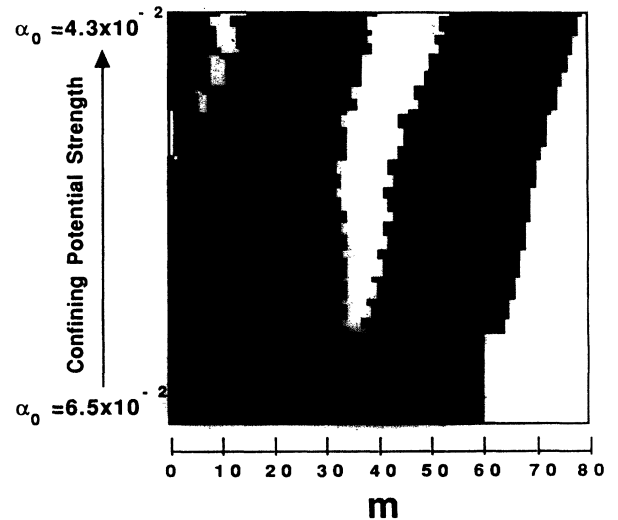


FIG. 11. Occupation number of the angular momentum states as a function of α_0 for $N_p = 60$, calculated within the Hartree-Fock approximation. The occupied orbits are represented in black and the unoccupied ones are shown in white.

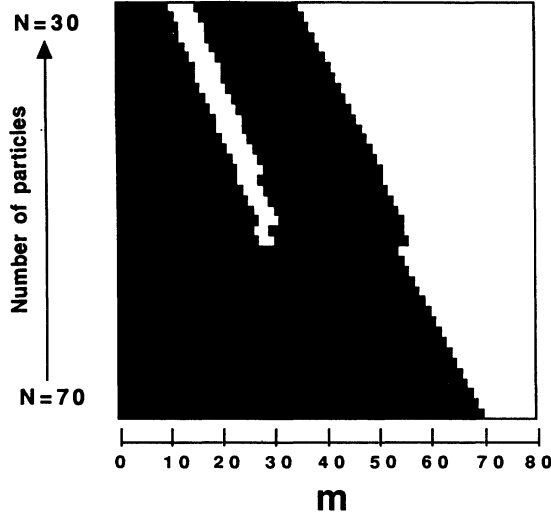


FIG. 12. Occupation number of the angular momentum states as a function of N_p for $\alpha_0 = 6.25 \times 10^{-2}$, calculated within the Hartree-Fock approximation.

all occupied levels should have a lower energy than the unoccupied ones.

We would like to point out that the exchange term is of key importance in order to have a compacted dot solution. Notice that we have assumed that occupation is nonzero only for the first Landau level and that the spins are fully polarized. One could argue that these assumptions alone can lead to a compacted drop, as a strong enough confining potential can always be chosen such that the ground state is the minimum total angular momentum solution even if one takes only the repulsive Hartree term. This would be possible because the particles would be squeezed to the center, without being able to occupy higher Landau levels, or flip spin (see Fig. 13,

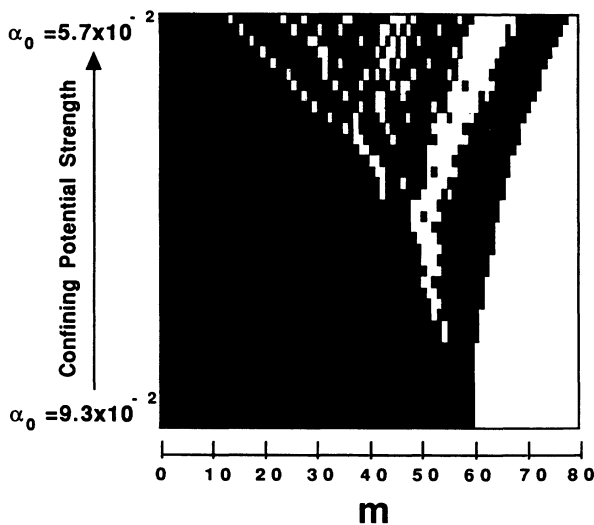


FIG. 13. Occupation number of the angular momentum states as a function of α_0 for $N_p = 10$, calculated within the Hartree approximation.

where we repeat the calculation for Fig. 11 without the exchange term). In reality, as we increase the confining potential, there are two mechanisms which tend to lower the total energy of the dot, one by compacting the particles to the low angular momentum orbits in the first Landau level, with polarized spins, and the other by moving particles to a higher Landau level or opposite spin polarization state. By increasing the confining potential we enhance both of these effects. Therefore, in order to have a $\nu = 1$ compacted dot we must have a window of α_0 that allows totally packed dots with no higher Landau level occupation. It is here that exchange comes in play, providing an attractive interaction that lowers the bound on α_0 to have a compacted dot, which opens that window.

The ideas above can be expressed quantitatively. The lower bound on α_0 , i.e., the minimum confining strength necessary to keep an N_p -particle dot compacted, can be obtained as follows. Within the Hartree approximation, α_0^{\min} is obtained from the condition that the net electric field on the edge of the dot due to the electrons just balances the field due to the confining potential. The radial field due to the electrons diverges logarithmically, $E_r \propto \frac{e}{\epsilon l_B^2} \ln(R/\lambda_c)$, where R is the radius of the droplet and λ_c is an ultraviolet cutoff length scale. The field due to the confining potential is $E_r = -\frac{e}{\epsilon l_B^2} \alpha_0 R/l_B$, so we find that $\alpha_0^{\min} \propto N_p^{-1/2} \ln(\frac{N_p}{\lambda_c^2/2l_B^2})$. Indeed, this dependence of α_0 on N_p fits very well the numerical results obtained when the exchange term is omitted (Hartree approximation), where we find $\alpha_0^{\min} \sim 0.118 N_p^{-1/2} \ln(\frac{N_p}{0.16})$ [see Fig. 14(a)]. We find that a similar function dependence on N_p reasonably fits the results obtained within the Hartree-Fock approximation, with $\alpha_0^{\min} \sim 0.083 N_p^{-1/2} \ln(\frac{N_p}{0.21})$ for our range of N_p [Fig. 14(b)]. Notice that the attractive exchange term has the tendency to keep the dot compacted, lowering the value of α_0^{\min} .

The upper bound on α_0 can be obtained by estimating the energy decrease of moving one particle from the edge to the center. The electrostatic energy of a disk of radius R and density $\rho_0 = \frac{e}{2\pi l_B^2}$ is $\mathcal{E}_{\text{disk}} = \frac{e^2}{\epsilon l_B} \frac{2}{3\pi} (R/l_B)^3$, which gives an estimate for the electrostatic energy of adding one electron to the edge of the dot of $\delta\mathcal{E}_{\text{edge}} = \frac{e^2}{\epsilon l_B} \frac{2\sqrt{2}}{\pi} \sqrt{N_p}$. The electrostatic energy cost of adding an electron to the center of the disk is $\delta\mathcal{E}_{\text{center}} = \frac{e^2}{\epsilon l_B} \sqrt{2} \sqrt{N_p}$. The total decrease in energy of moving one particle from the edge to the center is $\Delta\mathcal{E} = \frac{e^2}{\epsilon l_B} (\alpha_0 N_p - \frac{\pi-2}{\pi} \sqrt{2} \sqrt{N_p})$, which has to be $< \hbar\omega_c$ (or $< \mathcal{E}_{\text{Zeeman}}$) if we want to have occupation solely in the first Landau level (or with polarized spins). So we find $\alpha_0^{\max} \sim \frac{\pi-2}{\pi} \sqrt{2} N_p^{-1/2} + \frac{\hbar\omega_c}{e^2/\epsilon l_B}$ (or $\frac{\mathcal{E}_{\text{Zeeman}}}{e^2/\epsilon l_B}$) N_p^{-1} . The last term contains the ratio between the cyclotron (or Zeeman) and Coulomb energies. The condition for a compacted dot is $\alpha_0^{\min} < \alpha_0 < \alpha_0^{\max}$. For GaAs $\frac{\hbar\omega_c}{e^2/\epsilon l_B} \sim 0.4\sqrt{B}$, with B the magnetic field in Tesla. So for reasonable values of B and N_p in a dot, the term $N_p^{-1/2}$ in α_0^{\max} is the dominant one, which constrains the maximum possible N_p to the one that makes $\alpha_0^{\min} \sim \alpha_0^{\max}$, which gives $N_p^{\max} \sim 106$. If we use the value for α_0^{\min} given by the Hartree term alone we find

$N_p^{\max} \sim 12$. Although these values are rough estimates, they should make it clear that the attractive exchange term plays a major role in opening up a window in α_0 for which there is a compacted dot solution.

We have also performed the Hartree-Fock calculation for spin 1/2 electrons with Zeeman energy $\mathcal{E}_{\text{Zeeman}} \rightarrow 0_+$ (simply to break the degeneracy between the two spin polarized configurations). For large confining potentials, both spin-up and -down electrons form compact droplets of filling fraction $\nu = 1$. However, the droplet of, say, spin down electrons, is smaller and the electrons near the edge form a ferromagnetic state as pointed out in Ref. 8. As we decrease α_0 , the separation between the spin-up edge and the spin-down edge increases. At even smaller α_0 the spin-down electrons no longer form a compact droplet, which may be a sign of FQH states. As α_0 decreases below $\alpha_s \sim 0.53N_p^{-1/2} + 0.49N_p^{-1}$, all the electrons are spin polarized (the coefficient in $N_p^{-1/2}$ is approximately the same obtained from the electrostatic consideration and the one in N_p^{-1} shows the tendency of exchange to align spins as an effective Zeeman energy).

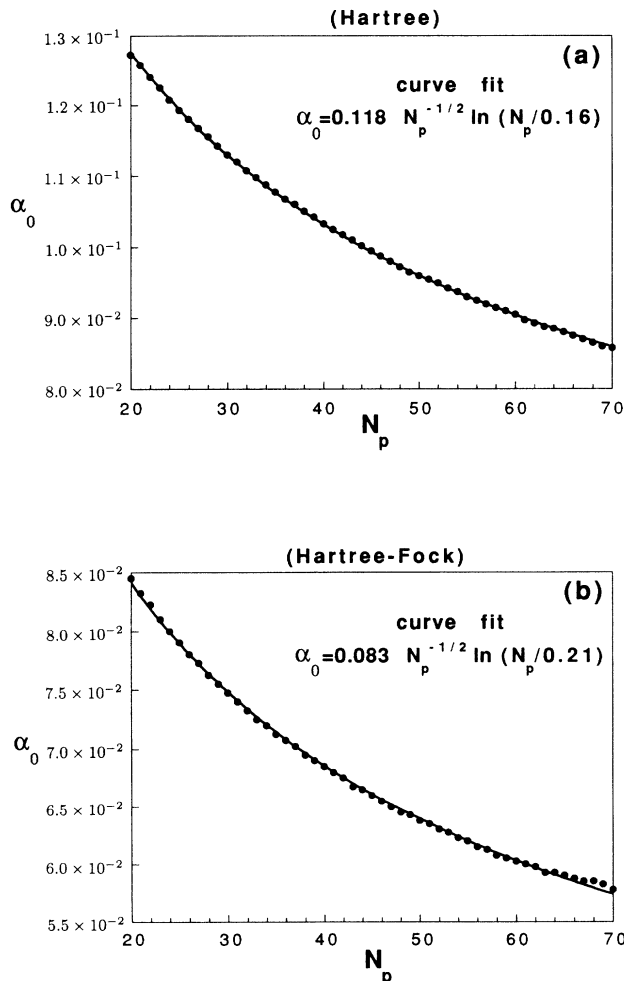


FIG. 14. Minimum α_0 necessary to keep an N_p -particle droplet compacted, calculated using the (a) Hartree and (b) Hartree-Fock approximations. The solid line is the best curve fit consistent with an electrostatic (Hartree) argument.

Thus for $\alpha_0^{\min} < \alpha_0 < \alpha_s$, the electrons form a spin polarized compact droplet. The exchange term tends to align the spins, increasing further the size of the window of α_0 's such that the droplet is compact.

We find that the inclusion of the exchange term brings into the picture effects that are left out from purely electrostatic models, which consider the effect of the Coulomb interaction via the direct term alone. The picture we describe here for the compact $\nu = 1$ droplet within the Hartree-Fock approximation seems to be consistent with exact calculations for systems with a small ($N = 6$) number of electrons,⁷ for a finite region of confining potential strengths. This is in the spirit of the calculations we presented in Sec. III, where the exact results we obtained for small systems support qualitatively the Hartree-Fock results.

The next question is how to experimentally obtain a value for α_0 that falls within the window above. In order to make the connection to real samples, we use the parabolic confining potential in Ref. 9. There they use $V_{\text{ext}}(r) = \frac{1}{2}m^*\omega^2 r^2$, with m^* the effective electron mass in GaAs and $\hbar\omega = 1.6$ meV for the particular device. The relation between our dimensionless α_0 (or alternatively, given in units of $\frac{e^2}{\epsilon l_B} = 1$ and $l_B = 1$) to this confining potential is obtained by equating $\alpha_0 \frac{e^2}{\epsilon l_B} l_B^{-2}$ to $m^*\omega^2$, which gives $\alpha_0 = \frac{(\hbar\omega)^2}{(e^2/\epsilon l_B)(\hbar\omega_c)}$, or $\alpha_0 \sim 0.376B^{-3/2}$, B in Tesla. For $N_p = 40$, for example, we find that $B = 2.5$ T will yield a value of α_0 in the allowed window, so that the dot occupation will be the one of a compacted $\nu = 1$ droplet. As we increase B beyond 3.1 T the edge will undergo a reconstruction.

We now turn into the possibility of probing experimentally the transition between a compacted and an expanded dot. In order to make a clear connection between this expansion effect and experimentally observable quantities, we describe below the implications of the effect to tunneling experiments into quantum dots. In resonant tunneling experiments, the energy difference between the ground states of an $N + 1$ and N electron system, $\mu(N)$, can be probed by tunneling in and out of the dot a single electron at a time, when the Fermi level of the electrodes become resonant with the quantum level of the dot.¹⁰⁻¹² By following a peak, the dependence of the chemical potential on the magnetic field can be observed. In Fig. 15 we calculated, within the Hartree-Fock approximation, this dependence of the chemical potential (in meV) on B (in Tesla) for dots with N_p from 35 to 38. The "sawtooth" for $B < 2.5$ T corresponds to spin-down electrons being flipped and moved from the center to the edge of the dot. This result can also be obtained with the *self-consistent* model of Ref. 9, where only the Hartree term is included. The region between roughly 2.5 T and 3 T is the window of magnetic fields for which the electrons form a compact $\nu = 1$ droplet. The "dislocation" near $B = 3$ T corresponds to the reconstruction of the electron number occupation, marking the transition from the compacted to the expanded configuration. The existence of the compacted $\nu = 1$ droplet and the transition (dislocation) cannot be predicted without the inclusion of the exchange in the model of the electron island.

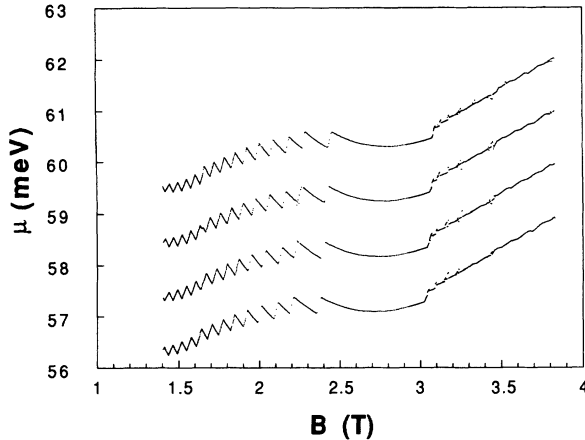


FIG. 15. Dependence on the magnetic field B of the energy cost to add one more particle μ to an island with 35 (lowest curve), 36, 37, and 38 (highest curve) electrons. The “sawtooth” corresponds to $1 < \nu < 2$, where electrons are spin flipped and taken from the center to the edge as the magnetic field is increased. The “dislocations” near $B \sim 3$ T correspond to the transition between compacted and separated dots. The region in between ($B \sim 2.5$ – 3 T) is the window for which the dot is a compact $\nu = 1$ droplet. These results were obtained for the parabolic confining potential of the sample studied in Ref. 9, with $\alpha_0 = 0.376B^{-3/2}$ (B in Tesla).

In addition to this anomaly in the peak position vs B , the expansion of the size of the dot will also increase its coupling to the probing leads, as this coupling depends on the distance between leads and island. The tunneling current should then increase for an expanded dot. In Fig. 16 we show the dependence of the size of the droplet (measured as the radius of the orbit of the outmost electron) on α_0 and on the number of particles N_p in the dot. In Fig. 16(a) we show the size of a 60 electron droplet as a function of α_0 and in Fig. 16(b) we fixed the value of α_0 and varied the number of electrons from 40 to 70. The effect on the amplitude of the resonant peak, together with the anomaly in the peak position, should be a signature that a transition is indeed occurring in the occupation density of the quantum dot.

V. THE EDGE MODES AFTER THE TRANSITION

As we have seen in the preceding sections, after smoothing the edge potential enough, a transition takes place, and the Fermi-liquid occupation density gives way to a more complex state. In terms of the electronic occupation distribution, the new state looks as if electrons start to deposit a certain distance away from the bulk of the QH liquid. The QH “puddle” that is formed, as mentioned above, brings in two more boundaries for each edge, and we then have three singularities. The interactions take charge in destroying the Fermi-liquid discontinuity, as the three singularities are finitely separated.

These three singularities can be related to three branches of gapless modes, which correspond to particle-

hole excitations near each of the singularities. An intuitive way to visualize the three branches is by considering the occupation number after the transition simply within the Hartree-Fock approximation, which would look as in Fig. 17. There the three edges are clearly identified. Correlations destroy the Fermi discontinuities, but we will still have the three Luttinger liquid singularities at the three Fermi points. Notice that the pair of branches that is added always has opposite chirality. An edge that had one right-moving branch before the transition, for example, will have two right-moving branches and one left-moving branch. All these three branches are strongly coupled. One clear experimental consequence of now having one branch moving in the opposite direction (the one left-moving branch in the originally right-moving edge, for example) is that one could probe such excitations,

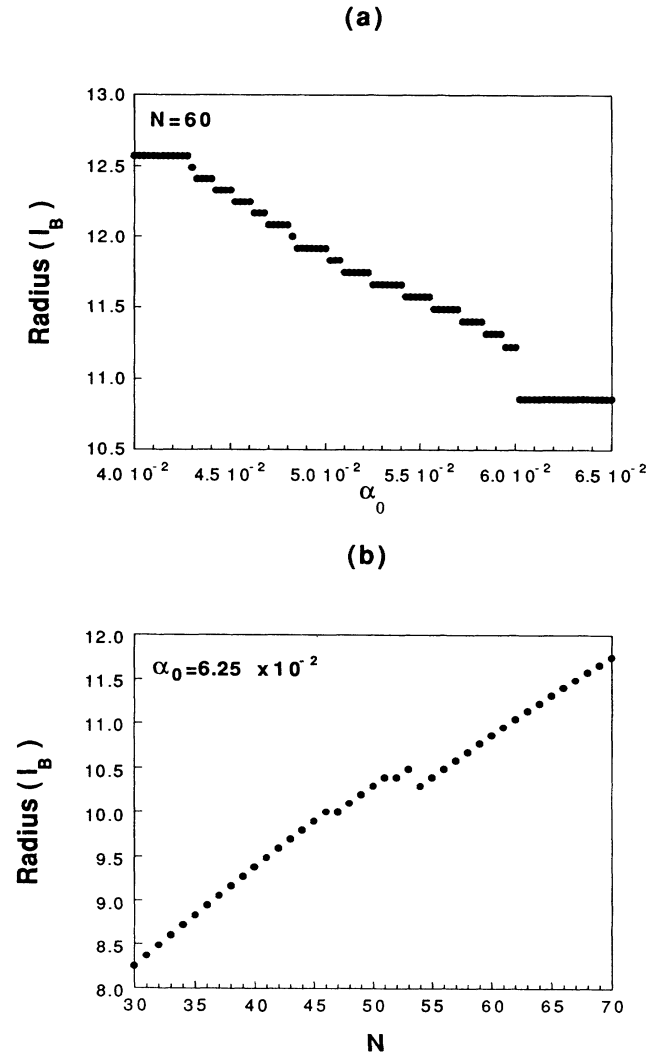


FIG. 16. Radius of the QH droplet for (a) fixed N_p and varying α_0 and (b) fixed α_0 and varying N_p . One can vary α_0 by changing the strength of the confining potential or by changing the magnetic field. For the parabolic confining potential of the sample studied in Ref. 9, the parameter $\alpha_0 = 0.376B^{-3/2}$ (B in Tesla).

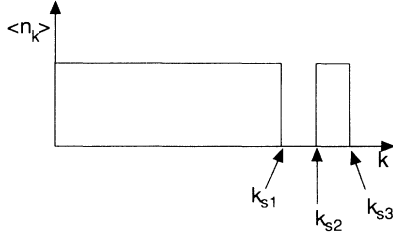


FIG. 17. Momentum occupation distribution after reconstruction, if calculated only within the Hartree-Fock approximation. The addition of two singularities correspond to the addition of two branches of opposite moving edge excitations.

where originally there was none. We will show, however, that the presence of impurities localize two of the three branches and such backpropagating modes cannot be observed beyond the localization length.

We will use the bosonized description of the edge states in the FQH regime presented in Ref. 13, which we summarize below for our particular case of $\nu = 1$. Let $\phi_{R,L}$ be two fields, described by the Lagrangian density

$$\mathcal{L}_{R,L} = \frac{1}{4\pi} \partial_x \phi_{R,L} (\pm \partial_t - v \partial_x) \phi_{R,L} \quad (16)$$

(v is the velocity of the excitations) and the equal-time commutation relations

$$[\phi_{R,L}(t, x), \phi_{R,L}(t, y)] = \pm i\pi \operatorname{sgn}(x - y). \quad (17)$$

Left- and right-moving electron operators can be written as $\Psi_{R,L}(x, t) \equiv e^{\pm i\phi_{R,L}(x, t)}$, which can be shown to satisfy the correct anticommutation relations.¹⁴ The electron density is given by $\rho_{R,L} = \partial_x \phi_{R,L}$ and the Hamiltonian is

$$H_{R,L} = \frac{v}{4\pi} \int dx \rho_{R,L}^2. \quad (18)$$

Consider three edge branches as depicted in Fig. 18, labeled by $i = 1, 2, 3$. We can generalize the description above to include several branches, writing the following Lagrangian density:

$$\mathcal{L} = \frac{1}{4\pi} \sum_{i,j} [K_{ij} \partial_t \phi_i \partial_x \phi_j - V_{ij} \partial_x \phi_i \partial_x \phi_j], \quad (19)$$

where the matrices K and V contain, respectively, information on the direction of propagation (chirality) of each branch and interactions between the branches (including a diagonal term containing the velocities). For this analysis let us assume two R branches (1 and 3) and one L branch (2) such that



FIG. 18. Three branches of edge excitations, two right moving (1 and 3, on the sides) and one left moving (2, in the center).

$$K = \begin{pmatrix} 1 & 0 & 0 \\ 0 & -1 & 0 \\ 0 & 0 & 1 \end{pmatrix}. \quad (20)$$

Electron operators can be written as

$$\Psi_L \propto \exp\left(i \sum_i l_i \phi_i\right), \quad (21)$$

$$l_i = \sum_j K_{ij} L_j, \quad (22)$$

where the L_i 's are integers satisfying $\sum_i L_i = 1$. The Lagrangian in (19) is not the most general one. We left out four fermion terms that cannot be written as the product of two densities. We know that it is the interactions between the densities that are responsible for changing the Fermi edge singularity and here we will concentrate on this particular effect of interactions. We have also assumed a local interaction in the densities. However, the long-range interaction can be easily included by allowing V_{ij} to have momentum dependence. In particular, the long-range Coulomb interaction contributes to a term $\sum_k \lambda_k (\sum_i \rho_{k,i}) (\sum_i \rho_{-k,i})$, where $\lambda_k \propto \ln k$ is the Fourier transformation of the $1/r$ Coulomb interaction and $\rho_{k,i}$ the Fourier component of the density of the i th branch. We see at long distances the most important interaction term is the one that involves only the total charge density $\sum \rho_i$. This contribution is

$$\frac{\lambda}{4\pi} \int dx \left(\sum_i \rho_i \right)^2 = \frac{\lambda}{4\pi} \int dx \sum_{i,j} \rho_i \rho_j, \quad (23)$$

which, when summed to the velocity terms, gives the total V matrix

$$V = \begin{pmatrix} v_1 + \lambda & \lambda & \lambda \\ \lambda & v_2 + \lambda & \lambda \\ \lambda & \lambda & v_3 + \lambda \end{pmatrix}. \quad (24)$$

Here, for simplicity, we have assumed that λ is a large constant independent of momentum. This will be the case if the Coulomb interaction is screened at a long distance (e.g., by gates nearby). We will focus primarily in the case where $\lambda \gg v$'s, i.e., strongly coupled branches. Also, if the system has particle-hole symmetry, then $v_1 = v_3$. We start by rewriting the Lagrangian (19) in terms of new fields $\tilde{\phi}_i = \sum_j U_{ij} \phi_j$ that simultaneously diagonalize K and V . Furthermore, we would like to keep, for convenience,

$$\tilde{K} = (U^T)^{-1} K U^{-1} = K \quad (25)$$

so that the commutation relations of the $\tilde{\phi}$'s are the same as the ones for the ϕ 's. The transformation matrix U for $\lambda \gg v$'s is

$$U_{\lambda \rightarrow 0} = \begin{pmatrix} 1 & 1 & 1 \\ \frac{1}{\sqrt{2}} & \sqrt{2} & \frac{1}{\sqrt{2}} \\ -\frac{1}{\sqrt{2}} & 0 & \frac{1}{\sqrt{2}} \end{pmatrix}. \quad (26)$$

The mode in the first line of U , $\tilde{\phi}_1 = \phi_1 + \phi_2 + \phi_3$, is

simply the total charge density mode (equivalently, $\tilde{\rho}_1 = \rho_1 + \rho_2 + \rho_3$, as $\rho = \partial_x \phi$). What we show next is that, once we add to the Lagrangian (19) electron scattering terms due to the presence of impurities, this total charge mode is left unperturbed, and the other two will localize.

The scattering terms between electron operators in the three edges that can be added to the Lagrangian are bosonic couplings with zero charge. These can be written as $T_L = \exp(i \sum_i l_i \phi_i) = \exp(i \sum_{ij} L_i K_{ij} \phi_j)$, where now the L_i 's are integers satisfying $\sum_i L_i = 0$ (T_L is bosonic and neutral). In terms of the rotated fields $\tilde{\phi}$'s, $T_L = \exp(i \sum_i \tilde{l}_i \tilde{\phi}_i)$, where $\tilde{l}_i = \sum_j l_j U_{ji}^{-1}$. Let us fo-

cus on the most relevant T_L 's; the naive renormalization group (RG) dimension can be obtained from the T_L correlations

$$\begin{aligned} & \langle T_L^\dagger(t=0, x) T_L(t=0, x=0) \rangle \\ & \propto \exp \left(- \sum_{i,j} \tilde{l}_i \tilde{l}_j \langle \tilde{\phi}_i(t=0, x) \tilde{\phi}_j(t=0, x=0) \rangle \right) \\ & \propto x \exp \left(- \sum_i \tilde{l}_i^2 \right) = x^{-\gamma_L}. \end{aligned} \quad (27)$$

Writing γ_L in terms of the L 's we obtain

$$\begin{aligned} \gamma_L &= \sum_i \tilde{l}_i^2 = \tilde{l}^T \tilde{l} = l^T U^{-1} (U^{-1})^T l = L^T K U^{-1} (U^{-1})^T K L \\ &= L^T U^T (U^T)^{-1} K U^{-1} (U^{-1})^T K U^{-1} U L = L^T U^T \tilde{K}^2 U L = L^T (U^T U) L, \end{aligned} \quad (28)$$

where we used $\tilde{K}^2 = K^2 = I$. It is easy to show that the minima γ_L , with $\sum_i L_i = 0$, are given by

$$L = \pm \begin{pmatrix} 1 \\ -1 \\ 0 \end{pmatrix}, \quad L = \pm \begin{pmatrix} 0 \\ -1 \\ 1 \end{pmatrix}, \quad (29)$$

which correspond to T_L operators that transfer charges between the center branch (L) to the two side branches (R). In terms of the \tilde{l} 's, we have

$$\tilde{l} = (U^{-1})^T K L = K U L = \pm \begin{pmatrix} 0 \\ \frac{1}{\sqrt{2}} \\ -\frac{1}{\sqrt{2}} \end{pmatrix}, \quad \pm \begin{pmatrix} 0 \\ \frac{1}{\sqrt{2}} \\ \frac{1}{\sqrt{2}} \end{pmatrix}. \quad (30)$$

The Hamiltonian density with these most relevant T_L terms added is

$$\mathcal{H} = \mathcal{H}_0 + \mathcal{H}_T, \quad (31)$$

where

$$\mathcal{H}_0 = \frac{\tilde{v}_1}{4\pi} (\partial_x \tilde{\phi}_1)^2 + \frac{\tilde{v}_2}{4\pi} (\partial_x \tilde{\phi}_2)^2 + \frac{\tilde{v}_3}{4\pi} (\partial_x \tilde{\phi}_3)^2 \quad (32)$$

and

$$\mathcal{H}_T = \xi_+(x) e^{i \frac{\tilde{\phi}_2 + \tilde{\phi}_3}{\sqrt{2}}} + \xi_-(x) e^{i \frac{\tilde{\phi}_2 - \tilde{\phi}_3}{\sqrt{2}}} + \text{H.c.} \quad (33)$$

The ξ_\pm describe the random tunneling coupling due to impurities, with correlations $\langle \xi_\pm(x) \xi_\pm(y) \rangle = \Delta_\pm \delta(x-y)$.

Notice that $\tilde{\phi}_1$ remains free, as the added tunneling terms do not depend on it. This one component (total charge, as $\tilde{\rho}_1 = \rho_1 + \rho_2 + \rho_3$) behaves just like the one branch before the transition. The other two, we will argue below, should be localized because of the impurities.

Let $\tilde{\phi}_\pm = (\tilde{\phi}_2 \pm \tilde{\phi}_3)/\sqrt{2}$, which obey the commutation relations

$$\begin{aligned} & [\tilde{\phi}_\pm(t, x), \tilde{\phi}_\pm(t, y)] = 0, \\ & [\tilde{\phi}_\pm(t, x), \tilde{\phi}_\mp(t, y)] = -i\pi \text{sgn}(x-y). \end{aligned} \quad (34)$$

We can identify $\tilde{\Pi}_\pm = \frac{\partial_x \tilde{\phi}_\pm}{2\pi}$ as the conjugate momenta to $\tilde{\phi}_\pm$. We can rewrite the Hamiltonian for $\tilde{\phi}_2$ and $\tilde{\phi}_3$ in terms of $\tilde{\phi}_\pm$:

$$\begin{aligned} \mathcal{H}_{2,3} &= \frac{\tilde{v}}{4\pi} \left[(\partial_x \tilde{\phi}_+)^2 + (\partial_x \tilde{\phi}_-)^2 \right] \\ &+ \xi_+(x) e^{i\tilde{\phi}_+} + \xi_-(x) e^{i\tilde{\phi}_-} + \text{H.c.}, \end{aligned} \quad (35)$$

where we assume that $\tilde{v}_2 \approx \tilde{v}_3 \approx \tilde{v}$. This is a more complicated version of a sine-Gordon (SG) Hamiltonian density with position dependent coupling, as it involves self-interactions in both a field and its conjugate momentum.

If we had only one of ξ_+ or ξ_- , we would have a Hamiltonian for a simple SG with position dependent coupling, which we could write as

$$\mathcal{H} = \frac{\tilde{v}}{4\pi} \left[(2\pi\tilde{\Pi})^2 + (\partial_x \tilde{\phi})^2 \right] + \xi(x) e^{i\tilde{\phi}} + \text{H.c.} \quad (36)$$

Working in units of $\tilde{v} = 1$, and rescaling the fields as $\Pi' = \sqrt{2\pi}\tilde{\Pi}$ and $\phi' = \tilde{\phi}/\sqrt{2\pi}$ (which keep the commutation relations unchanged), we have

$$\mathcal{H} = \frac{1}{2} \left[\Pi'^2 + (\partial_x \phi')^2 \right] + \xi(x) e^{ig\phi'} + \text{H.c.}, \quad (37)$$

with $g = \sqrt{2\pi}$. This problem, equivalent to a Coulomb gas with position dependent chemical potential, was studied in Refs. 15 and 16. The impurity coupling Δ_\pm is relevant for $g < \sqrt{6\pi}$ (in the constant coupling constant or chemical potential Coulomb gas, the condition is $g < \sqrt{8\pi}$). This is indeed our case, and therefore the presence of impurities localizes the other two branches of excitations represented by $\tilde{\phi}_2$ and $\tilde{\phi}_3$.

Notice that what we have done above is equivalent to understanding the RG flows in the planes $\Delta_+ = 0$ and $\Delta_- = 0$, and this implies Δ_\pm are relevant in all directions around $\Delta_\pm = 0$ if $g < \sqrt{6\pi}$. The RG flows to a strong fixed point when both $\Delta_\pm \neq 0$. It is possible that this strong fixed point is a localized state, motivated by the flow when $\Delta_- = 0$. The properties of this strong fixed point will be the subject of further studies.

VI. TUNNELING INTO RECONSTRUCTED EDGES

The formalism in the preceding section can be used to study the electron tunneling into the reconstructed edges. The electron propagator in time in general has a form

$$\langle c^\dagger(t)c(0) \rangle \propto \frac{1}{t^{\gamma_L}}$$

with γ_L given in Eq. (28). But now the L_i 's satisfy $\sum_i L_i = 1$. In the limit $\lambda/v \gg 1$, U is given by Eq. (26). The minimum exponent is $\gamma_L = 1$ (the Fermi-liquid value) for electrons described by $L = (1, -1, 1)$. This configuration corresponds to adding two electrons on the two side branches and removing one electron from the center branch. Adding a single electron to the side branch leads to a exponent $\gamma_L = 2$ and to the center branch $\gamma_L = 3$.

Let us consider tunneling between two reconstructed edges. At very low temperatures and low voltages, the electron with the configuration $L = (1, -1, 1)$ will dominate the tunneling and leads to a linear $I - V$ curve,¹⁷ since $I \propto V^{2\gamma_L-1}$ and $\gamma_L = 1$. At higher voltages, depending on the sample geometry, it may be easier for an electron to just tunnel into the side branch [with configuration $L = (1, 0, 0)$]. In this case $I \propto V^3$ and $(dI/dV)_{V=0} \propto T^2$.

The above discussion also applies to the reconstructed edges of Laughlin states of filling fraction $1/m$. But now for the $L = (1, -1, 1)$ electron the exponent $\gamma_L = m$. $\gamma_L = 2m$ for $L = (1, 0, 0)$ and $\gamma_L = 3m$ for $L = (0, 1, 0)$. We see that in the limit $\lambda/v \gg 1$ the minimum exponent in the electron propagator is not affected by the edge reconstruction. This result is valid even when more than one pair of edge branches is generated. This is because adding electrons of configuration $L = (1, -1, 1, -1, \dots, 1)$ just displaces all the edge branches by the same amount. Thus the electron of $L = (1, -1, 1, -1, \dots, 1)$ just couples to the total density $\sum \rho_i$ and does not couple to other neutral modes. In the limit $\lambda/v \gg 1$, the total density mode decouples from other neutral modes. This is the reason why the $L = (1, -1, 1, -1, \dots, 1)$ electron always has the exponent $\gamma_L = m$. We would like to stress that the above result is valid only at low energies (energies below the smallest Fermi energy of generated edge branches). The high energy behavior of the electron propagator is not clear. In that case it is probably better to view the edge region as a compressible gas.

For tunneling between two reconstructed FQH edges,

we expect $I \propto V^{2m-1}$ and $(dI/dV)_{V=0} \propto T^{2m}$ at low voltages and low temperatures. This is consistent with a recent experiment on tunneling between (smooth) edges of $1/3$ FQH states.¹⁸

VII. CONCLUSION

In this paper we studied the electronic density of quantum Hall liquids, focusing on short length scales that are comparable with the magnetic length. We found that sharp electronic occupation densities, corresponding to a $Z_F = 1$ Fermi liquid, are possible because of the chiral nature of the system. This sharp distribution is stable against variations in the confining potential up to a certain point, beyond which it undergoes a transition and electrons start to separate from the bulk and deposit a distance $\sim 2l_B$ away. The transition is shown to be qualitatively described within the Hartree-Fock approximation. The separation generates a pair of branches of edge states that move in opposite directions.

For even smoother confining potentials more pairs of edge branches may be generated which eventually leads to the compressible liquid picture. However, at low energies we see that the edge theory for sharp edges can also be used to describe the smooth edges (i.e., the reconstructed edges) once the additional pairs of edge branches are included. This result agrees with the picture obtained from a general consideration.¹³ In particular the algebraic exponent in the tunneling I-V curve is not affected by edge reconstruction in the presence of long-range interactions.

We would like to remark that the separated electrons do not form any fractional quantum Hall state. This is because the separation between the Fermi edges is always of order magnetic length for realistic potentials. In this case $1/3, 1/5, \dots$ states are all described by Luttinger liquid and are indistinguishable.

We also presented results for quantum dots, where we predict that this effect of edge separation can be related to an expansion of the dot, which could be experimentally observed.

ACKNOWLEDGMENTS

The authors would like to thank Dmitrii Chklovskii, Yong Baek Kim, David Abusch, Olivier Klein, Paul Belk, Marc Kastner, and Ray Ashoori for useful discussions. This work was supported by the NSF Grant No. DMR-91-14553.

¹ L. P. Kouwenhoven, B. J. van Wees, N. C. van der Vaart, C. J. P. M. Harmans, C. E. Timmering, and C. T. Foxon, *Phys. Rev. Lett.* **74**, 685 (1990).

² A. M. Chang, *Solid State Commun.* **74**, 871 (1990).

³ C. W. J. Beenakker, *Phys. Rev. Lett.* **64**, 216 (1990).

⁴ D. B. Chklovskii, B. I. Shklovskii, and L. I. Glazman, *Phys. Rev. B* **46**, 4026 (1992).

⁵ B. Y. Gelfand and B. I. Halperin (unpublished).

⁶ A. H. MacDonald, S. R. Eric Yang, and M. D. Johnson, *Aust. J. Phys.* **46**, 345 (1993)

⁷ S. R. Eric Yang, A. H. MacDonald, and M. D. Johnson (unpublished).

⁸ J. Dempsey, B. Y. Gelfand, and B. I. Halperin, *Phys. Rev. Lett.* **70**, 3639 (1993).

- ⁹ P. L. McEuen, E. B. Foxman, Jari Kinaret, U. Meirav, M. A. Kastner, Ned S. Wingreen, and S. J. Wind, *Phys. Rev. B* **45**, 11 419 (1992).
- ¹⁰ Bo Su, V. J. Goldman, and J. E. Cunningham, *Science* **255**, 313 (1992).
- ¹¹ P. L. McEuen, E. B. Foxman, U. Meirav, M. A. Kastner, Yigal Meir, Ned S. Wingreen, and S. J. Wind, *Phys. Rev. Lett.* **66**, 1926 (1991).
- ¹² R. C. Ashoori, H. L. Stormer, J. S. Weiner, L. N. Pfeiffer, and K. W. West, *Phys. Rev. Lett.* **68**, 3088 (1992).
- ¹³ Xiao-Gang Wen, *Intl. J. Mod. Phys. B* **6**, 1711 (1992).
- ¹⁴ R. Floreanini and R. Jackiw, *Phys. Rev. Lett.* **59**, 1873 (1988).
- ¹⁵ W. Apel, *J. Phys. C* **15**, 1973 (1982).
- ¹⁶ T. Giamarchi and H. J. Shulz, *Europhys. Lett.* **3**, 1287 (1987).
- ¹⁷ Xiao-Gang Wen, *Phys. Rev. B* **44**, 5708 (1991).
- ¹⁸ F. Milliken and R. Webb (private communication).

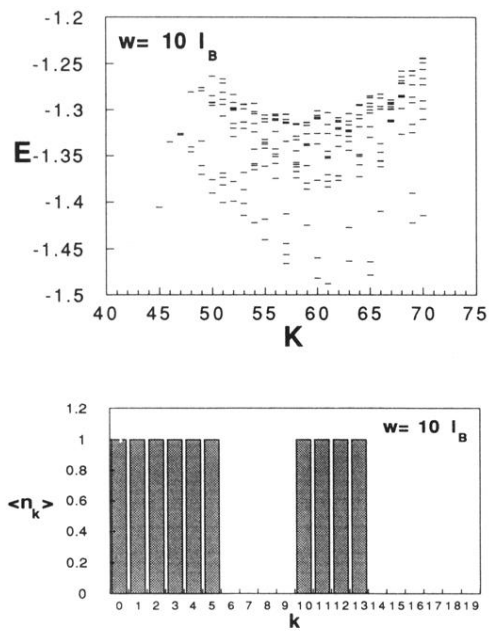


FIG. 10. Energy levels and occupation numbers for $w = 10l_B$ calculated within the Hartree-Fock approximation (the hopping or off-diagonal elements were suppressed).

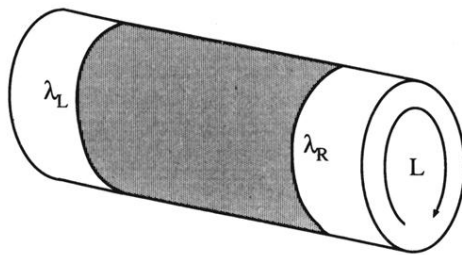


FIG. 3. Cylindrical geometry, equivalent to a strip of length L and periodic boundary conditions, where it is convenient to use the Landau gauge. The QH liquid (shaded area) lies on the surface of the cylinder, between its left and right edges at λ_L and λ_R .

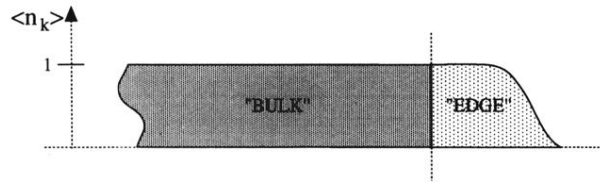


FIG. 4. The $\nu = 1$ droplet is divided into “bulk,” where all the states are fully occupied, and “edge,” in which states can be partially occupied. The division allows one to focus the computations solely on the edge electrons, with the bulk simply contributing to the one particle dispersion. This sort of division is not unique, as one can adjust the position of the boundary between the two regions; this boundary can be moved as long as the sites on the edge side of it are all fully occupied.

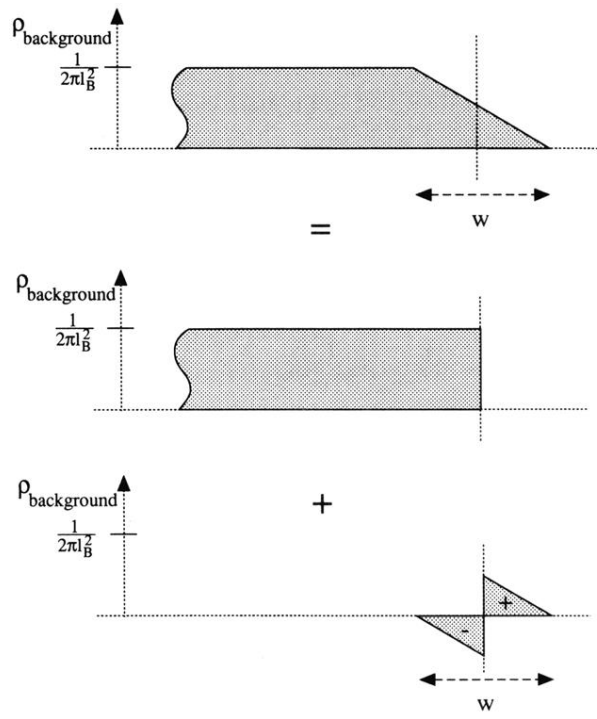


FIG. 5. Smoothed background charge density, which over a width w drops from its bulk value to zero. Such density can be written as the superposition of a sharp density profile to a dipole term, which is used to tune the confining potential as function of w .

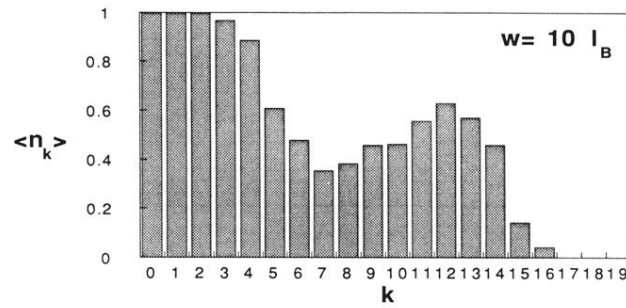
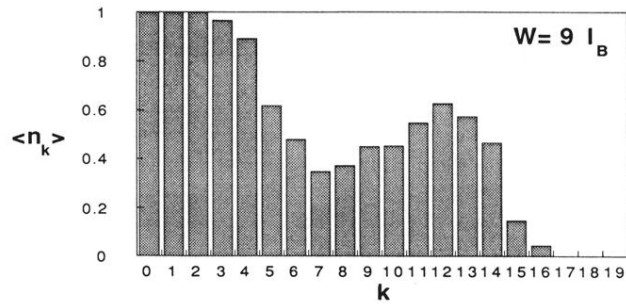


FIG. 8. Occupation numbers for the ground state past the transition, for $w = 9l_B$ and $10l_B$. Notice how a lump of density moves away from the main body of QH fluid. This density profile (which goes from its bulk value to zero by first decreasing, then increasing, and finally decreasing again) is the signature of the existence of now three singularities, and thus three branches of edge excitations.